European Journal of Neurology

european journal of neurology
the official journal of the european academy of neurology

REVIEW ARTICLE OPEN ACCESS

Corneal Confocal Microscopy to Diagnose Peripheral Neuropathy: A Systematic Review and Meta-Analysis

Ioannis N. Petropoulos[1] | Omar A. Madani[1] | Hoda Y. Gad[1] | Ziyad R. Mahfoud[2,3] | Georgios Ponirakis[1] | Ross MacDonald[4] | Rayaz A. Malik[1,5]

[1]Research Division, Weill Cornell Medicine-Qatar, Doha, Qatar | [2]Division of Medical Education, Weill Cornell Medicine, Doha, Qatar | [3]Division of Epidemiology, Department of Population Health Sciences, Weill Cornell Medicine, New York, New York, USA | [4]Health Sciences Library, Weill Cornell Medicine-Qatar, Doha, Qatar | [5]Institute of Cardiovascular Medicine, University of Manchester, Manchester, UK

Correspondence: Rayaz A. Malik (ram2045@qatar-med.cornell.edu)

Received: 28 May 2025 | **Revised:** 24 September 2025 | **Accepted:** 9 October 2025

Funding: This work was supported by BMRP grant #20038654 from the Qatar Research Development Innovation Council. The statements made herein are solely the responsibility of the authors.

Keywords: biomarkers | diagnosis | neurology | neuropathology | neuropathy

ABSTRACT

Background and Objectives: Peripheral neuropathy (PN) may be diagnosed late or may remain undiagnosed. Studies have shown that measurement of corneal nerve fiber length (CNFL) using corneal confocal microscopy (CCM) may have diagnostic utility in diabetic and other peripheral neuropathies.

Methods: The main databases [CENTRAL, Embase (Ovid), and PubMed] were searched for peer-reviewed literature. Gray literature searching was undertaken using the ProQuest Dissertations & Theses database. The updated Preferred Reporting Items for Systematic Reviews and Meta-Analysis guidelines were used by two authors independently for screening and data extraction. The primary outcome of CNFL was represented by the standardized mean difference and 95% confidence interval, and differences between healthy controls (HC), patients with sub-clinical (PN−), and clinical (PN+) peripheral neuropathy were assessed. Sensitivity analysis was performed to assess the risk of bias.

Results: We identified $n = 52$ eligible studies ($n = 2995$ participants) reporting CNFL across 34 different conditions associated with PN. CNFL was significantly lower in PN+ patients compared to HC (standardized mean difference −1.12, 95% confidence interval −1.32 to −0.33, $p < 0.00001$), in PN− patients compared to HC (−0.78, −0.99 to −0.57, $p < 0.00001$), and in PN+ compared to PN− patients (−0.93, −1.53 to −0.33, $p = 0.002$). The results remained significant following sensitivity analysis to adjust for the risk of potential detection bias. The results remained significant independent of the choice of a random or fixed effects model.

Conclusions: This systematic review and meta-analysis shows that CNFL has utility in the diagnosis of peripheral neuropathies.

Abbreviations: AL amyloidosis, light chain amyloidosis; CCM, corneal confocal microscopy; CIDP, chronic inflammatory demyelinating polyradiculoneuropathy; CIPN, chemotherapy induced peripheral neuropathy; CMT1A, Charcot Marie Tooth type 1A; CNFL, corneal nerve fiber length; COVID-19, coronavirus disease 2019; GI, gastrointestinal (cancer); HC, healthy control; HIV, human immunodeficiency virus; HTA, hereditary transthyretin amyloidosis; ISFN, idiopathic small fiber neuropathy; NF1, neurofibromatosis type 1; NGF-β, nerve growth factor-β; OSA, obstructive sleep apnea; PN, peripheral neuropathy; SLE, systemic lupus erythematosus; TAO, thyroid disease associated ophthalmopathy; TFAP, transthyretin familial amyloid polyneuropathy.

1 | Introduction

Peripheral neuropathy (PN) has varied etiology, symptomatology, and severity [1]. Small fiber neuropathy is a common underpinning of PN [2]. Early identification of small nerve fiber dysfunction/damage is key in diagnosis, prognosis, and the assessment of the effectiveness of treatment [3]. A substantial body of evidence indicates that corneal confocal microscopy (CCM), a non-invasive ophthalmic imaging technique, can identify small nerve fiber degeneration. Specifically, corneal nerve fiber length (CNFL) of the subbasal nerve plexus provides an objective and repeatable measurement of small nerve fiber damage and repair (Figure S1). Corneal subbasal nerve fibers are sensory C-fibers originating from the trigeminal ganglion and are anatomically similar to intraepidermal nerve fibers in the skin [4]. We first reported a reduction in CNFL in patients with sub-clinical diabetic neuropathy, which increased with neuropathic severity and was related to clinical symptoms and signs [5, 6]. Since then, others have also employed CCM to show a lower CNFL in patients with PN from inflammatory, idiopathic, metabolic, autoimmune, toxic, genetic, and infectious causes [7]. The magnitude of difference in CNFL varies between studies, partly due to disease subtypes and stage, cohort size, and quantification method. We have conducted a systematic review and meta-analysis of studies utilizing CNFL in patients with PN and healthy controls.

2 | Methods

2.1 | Data Sources

This systematic review and meta-analysis is reported in accordance with the PRISMA guidelines [8]. The protocol was registered with the International Prospective Register of Systematic Reviews (PROSPERO) on 3/4/2022 (CRD42022289463). The CENTRAL, Embase (Ovid, 1988–present), and PubMed databases were chosen for searching peer-reviewed literature by an experienced librarian (RMD). Searches in CENTRAL and PubMed included Mesh subject headings and keywords, while the search in Embase included Emtree terms and keywords. Gray literature searching was undertaken using the ProQuest Dissertations and Theses (2004–present) database (Table S1). No limits, such as year, study type, or language, were applied. All searches were adapted from a previous systematic review and meta-analysis [9]. They were initially performed on 21 February 2022, then updated on 19 December 2022, and finally on 18 June 2023. Results from all searches were uploaded to the Covidence systematic review management platform (https://covidence.org/) and duplicates were removed.

Observational studies meeting the following criteria were included: (1) reporting on CNFL in PN or systemic diseases known to be associated with PN, (2) inclusion of an appropriate healthy control (HC) group (i.e., age- and/or sex-matched); (3) reporting statistical analysis between the respective study groups. The detailed characteristics of all included studies are presented in Tables 1–3. Studies were excluded if they were reporting on: (1) diabetic neuropathy; (2) central neurodegenerative diseases such as Parkinson's disease, multiple sclerosis, Alzheimer's disease, and stroke; (3) ophthalmic conditions such as lacrimal system, retinal, or corneal disorders, ocular surgery, or contact lens use; (4) lacking a healthy control group as a comparator; (5) clinical trials; (6) case reports; (7) case series; and (8) articles not written in English. Information on study location, disease, age, sex distribution, sample size, CNFL, CCM type, and analysis method was extracted directly from the published articles. A subgroup analysis was performed if ≥ 3 studies reported statistical analysis on CNFL between HC, patients with (PN+) and/or without (PN−) PN (Cochrane Handbook for Systematic Reviews of Interventions, chapter 10.11.3 Undertaking Subgroup Analysis). Data presented as median (range) were converted into mean ± SD using a web-based open calculator (accessible: https://www.math.hkbu.edu.hk/~tongt/papers/median2mean.html) based on established methodology [48–50]. Data presented as mean ± SEM were converted into mean ± SD using the Review Manager (RevMan) calculator.

2.2 | Study Selection

Following removal of duplicates, the remaining references were screened for relevance by two reviewers (I.N.P., H.G.) independently using the full citation, title, abstract, indexing terms, alongside the pre-specified inclusion and exclusion criteria. All studies not fulfilling the inclusion criteria were excluded, and full manuscripts of all eligible studies were obtained. Two independent reviewers (I.N.P., O.A.M.) made the final inclusion and exclusion decisions after reading the full articles, and in case of disagreement, a third reviewer (R.A.M.) was consulted for resolution. A data collection tool was developed, and data were extracted manually for each study by two reviewers (I.N.P., O.A.M.). If the required data were not available, the corresponding authors were contacted in writing. Studies were excluded if the corresponding author did not respond on three consecutive attempts 2 weeks apart or if they responded but were unable to provide the requested data. A flowchart of search results is provided in Figure 1.

2.3 | Data Extraction and Quality Assessment

The Cochrane Collaboration's tool was used to categorize the risk of bias into low, moderate, high, or unclear based on six domains, namely selection, performance, detection, attrition, reporting, and other bias. Quality assessment was undertaken by two reviewers (I.N.P., O.A.M.). If the risk of bias was deemed high or unclear, sensitivity analysis was performed to assess the effect of excluding the study, and the outcomes were reported.

2.4 | Unit Conversion

For studies [15, 18–20, 26, 28, 37, 38, 41, 43, 46] using alternative CNFL units, they were converted to mm/mm^2 based on the following formulas:

From μm/mm^2 to mm/mm^2.

- $(\mu m/mm^2) \times (1\,mm/10^3\,\mu m) = 1/10^3\,mm/mm^2$.

TABLE 1 | Characteristics of studies for HC versus PN+.

Study	Country	Condition	Age (years)		Sex (M/F)		CNFL (mm/mm^2)		CCM Model	Method
			HC	*PN+*	*HC*	*PN+*	*HC*	*PN+*		
Perini et al. [10]	Sweden	NGF-β Mutation	49.9	40.3	9/10	2/1	23.6 + 5.1	0.5 ± 0.8	HRT III RCM	CCMetrics
Pineiro et al. [11]	Spain	Fibromyalgia	40.3 ± 10.9	49.8 ± 12.6	7/12	3/12	13.9 ± 0.8	10.1 ± 1.0	HRT III RCM	ACCMetrics
Levy et al. [12]	France	Sjögren's syndrome	59.3 ± 12.3	58.9 ± 15.4	6/9	10/20	23.6 ± 4.2	12.4 ± 4.5	HRT III RCM	ImageJ
Tavakoli et al. (Appendix S1)	UK	ISFN	59.3 ± 3.9	57.5 ± 3.1	3/9	12/5	9.3 ± 1.9	4.4 ± 2.6	Confoscan P4	Tomey
Nortey et al. (Appendix S1)	USA	Sjögren's Syndrome	55.1 ± 13.0	67.2 ± 10.2	6/16	0/11	9.9 ± 2.4	4.3 ± 2.6	HRT III RCM	ACCMetrics
Ferdousi et al. (Appendix S1)	UK	GI Cancer	60.2 ± 8.7	63.8 ± 10.0	20/1	20/1	26.8 ± 4.3	18.1 ± 3.6	HRT III RCM	CCMetrics
Tavakoli et al. (Appendix S1)	UK	CMT 1A	43.0 ± 12.1	43.0 ± 12.1	7/5	6/6	26.7 ± 4.5	15.8 ± 5.2	HRT III RCM	*Not specified*
Wu et al. [13]	China	TAO	44.1 ± 7.2	43.5 ± 5.7	7/13	5/9	17.6 ± 3.6	10.4 ± 3.0	HRT III RCM	ACCMetrics
Mirza et al. [14]	Türkiye	COVID-19	35.5 ± 6.5	36.7 ± 8.3	16/6	12/12	17.8 ± 3.3	11.6 ± 2.9	HRT III RCM	ImageJ
Çalık et al. [15]	Türkiye	Vitamin D deficiency	41.1 ± 12.3	36.4 ± 12.9	3/11	9/19	1.4 ± 0.3	0.98 ± 0.20	HRT III RCM	ImageJ
Oudejans et al. [16]	Netherlands	Sarcoidosis	60.7 ± 2.9	49.5 ± 9.1	32/22	31/27	22.6 ± 7.3	13.6 ± 0.2	HRT III RCM	ACCMetrics
D'Onofrio et al. (Appendix S1)	UK	Hypertriglyceridemia	50.1 ± 14.0	43.9 ± 12.6	10/9	22/2	26.7 ± 4.4	19.2 ± 4.3	HRT III RCM	CCMetrics
Sharma et al. (Appendix S1)	UK	Hypothyroidism	45.0 ± 14.3	49.6 ± 13.3	8/12	9/11	14.2 ± 2.5	10.1 ± 2.3	HRT III RCM	CCMetrics
Khan et al. [17]	Pakistan	β-Thalassemia	19.2 ± 5.2	17.7 ± 3.8	9/11	9/11	27.0 ± 4.1	19.5 ± 4.9	HRT III RCM	ImageJ
Matsumoto et al. [18]	Japan	Sjögren's Syndrome	68.8 ± 9.8	65.4 ± 11.4	0/13	0/23	1.8 ± 0.4	1.2 ± 0.4	HRT III RCM	ImageJ
Kocayeboglu et al. [19]	Türkiye	IgG4-Related Disease	52.8 ± 9.1	50.1 ± 14.2	5/5	5/5	11.7 ± 3.8	7.0 ± 1.9	Confoscan3	ImageJ
Schneider et al. [20]	Germany	CIDP	71.3 ± 8.4	63 ± 12	9/6	10/6	23.5 ± 3.6	18.1 ± 3.4	HRT III RCM	ImageJ
Marshall et al. [21]	UK	Fibromyalgia	42.6 ± 11.8	45.4 ± 15.0	1/9	1/14	16.0 ± 3.0	12.3 ± 2.0	HRT III RCM	ACCMetrics
Brines et al. [22]	Netherlands	Sarcoidosis	46.2 ± 16.9	50.2 ± 10.0	25/23	31/32	17.1 ± 3.2	12.7 ± 2.9	HRT III RCM	ACCMetrics
Luzu et al. [23]	France	Sjögren's syndrome	50.9 ± 21.8	67.1 ± 7.9	6/14	2/17	20.5 ± 3.1	15.0 ± 5.2	HRT III RCM	ImageJ
Kolkedi et al. [24]	Hungary	COVID-19	46.7 ± 17.6	43.3 ± 13.8	11/17	18/17	13.0 ± 3.1	8.6 ± 3.7	HRT III RCM	ACCMetrics
Chiang et al. [25]	Australia	CIPN	54.7 ± 12.6	61.9 ± 10.7	9/16	14/6	17.4 ± 3.6	13.1 ± 3.2	HRT III RCM	ACCMetrics
Pagovich et al. (Appendix S1)	USA	Friedreich Ataxia	24.9 ± 4.0	24.7 ± 3.8	6/8	11/12	22.0 ± 3.5	15.4 ± 5.9	HRT III RCM	CCMetrics
Tepelus et al. [26]	USA	Sjögren's Syndrome	59.3 ± 12.7	57.5 ± 8.6	1/6	1/21	17.0 ± 4.3	9.76 ± 6.2	HRT III RCM	ImageJ
Zhang et al. [27]	China	TFAP	48.7 ± 16.0	40.8 ± 11.4	12/3	7/3	22.5 ± 3.2	18.4 ± 3.6	HRT III RCM	ImageJ

(Continues)

TABLE 1 | (Continued)

Study	Country	Condition	Age (years)		Sex (M/F)		CNFL (mm/mm^2)		CCM Model	Method
Turan et al. [28]	Türkiye	Fibromyalgia	42.0 ± 8.5	45.1 ± 6.8	0/42	0/34	15.9 ± 6.1	9.8 ± 3.8	Confoscan3	ImageJ
Thimm et al. [29]	Germany	HT Amyloidosis	62.7 ± 1.7	64.1 ± 2.9	15/5	15/5	17.4 ± 4.2	13.0 ± 3.5	HRT III RCM	ACCMetrics
Seeliger et al. [30]	Germany	Sjögren's Syndrome	61.5 ± 1.6	64.0 ± 4.0	1/5	11/15	14.6 ± 1.5	10.6 ± 3.9	HRT III RCM	ACCMetrics
Seeliger et al. [30]	Germany	CIDP	61.5 ± 1.6	67.0 ± 3.5	1/5	23/6	14.6 ± 1.5	10.9 ± 3.6	HRT III RCM	ACCMetrics
Bitirgen et al. (Appendix S1)	Türkiye	Rheumatoid arthritis	52.0 ± 13.1	52.1 ± 9.7	10/25	13/37	22.4 ± 3.5	18.5 ± 4.0	HRT III RCM	CCMetrics
Kemp et al. [31]	UK	HIV	53.8 ± 10.5	57.7 ± 7.8	20/0	14/0	27.2 ± 5.8	22.2 ± 3.6	HRT III RCM	CCMetrics
Thimm et al. [32]	Germany	AL Amyloidosis	62.9 ± 58.2	61.1 ± 39.8	14/7	14/7	17.5 ± 3.6	14.0 ± 3.4	HRT III RCM	ACCMetrics
Aykut et al. (Appendix S1)	Türkiye	Interstitial Cystitis	44.9 ± 11.5	50.1 ± 10.6	1/31	1/29	17.5 ± 2.6	11.3 ± 8.7	HRT III RCM	ACCMetrics
Chiang et al. [33]	Australia	CIPN	52.1 ± 14.0	58.7 ± 10.4	2/27	2/18	16.4 ± 4.0	12.9 ± 3.0	HRT III RCM	ACCMetrics
Marenco et al. [34]	Italy	Fabry Disease	32.5 ± 11.1	45.8 ± 18.7	7/8	6/5	11.8 ± 3.7	8.5 ± 2.9	HRT III RCM	ImageJ
Bitirgen et al. (Appendix S1)	Türkiye	Fabry Disease	34.5 ± 13.2	34.6 ± 13.5	10/7	10/7	19.5 ± 4.4	15.9 ± 3.4	HRT III RCM	CCMetrics
Keskiner-Ozturk et al. (Appendix S1)	Türkiye	CIDP	44.2 ± 12.4	50.5 ± 7.2	13/19	8/7	16.0 ± 3.1	12.8 ± 4.4	HRT III RCM	ACCMetrics
Chiang et al. [35]	Australia	CIPN	58.9 ± 7.9	60.8 ± 9.5	17/23	21/18	16.3 ± 3.2	13.7 ± 2.9	HRT III RCM	ACCMetrics
Chiang et al. [36]	Australia	CIPN	52.1 ± 13.5	56.4 ± 12.5	1/14	2/38	16.8 ± 3.7	13.6 ± 3.8	HRT III RCM	ACCMetrics
Turan et al. [37]	Türkiye	Myasthenia Gravis	32.0 ± 10.8	38.9 ± 14.6	8/12	8/13	14.2 ± 2.5	12.2 ± 2.3	Confoscan3	ImageJ
Kocayeboglu et al. [38]	Türkiye	Graves' Disease	33.8 ± 10.3	35.4 ± 11.2	14/26	11/29	8.9 ± 4.7	6.0 ± 2.5	Confoscan3	ImageJ
Chiang et al. [36]	Australia	CIPN	58.8 ± 11.5	59.8 ± 8.8	9/6	17/13	16.3 ± 4.7	13.9 ± 2.5	HRT III RCM	ACCMetrics
Szalai et al. [39]	Hungary	Systemic Sclerosis	64.6 ± 9.5	67.7 ± 9.4	15/15	5/28	11.6 ± 3.9	9.0 ± 3.9	HRT III RCM	ACCMetrics
Egenolf et al. [40]	Germany	SFN	47.5 ± 11.3	51.4 ± 12.9	13/54	21/34	14.9 ± 3.1	12.9 ± 3.3	HRT III RCM	*Not specified*
Bitirgen et al. (Appendix S1)	Türkiye	SLE	35.0 ± 13.7	33.7 ± 12.7	4/26	3/36	22.8 ± 4.1	20.4 ± 4.2	HRT III RCM	CCMetrics
Bitirgen et al. (Appendix S1)	Türkiye	Behcet's Disease	41.2 ± 11.5	39.9 ± 11.2	10/20	17/32	18.5 ± 4.1	16.3 ± 4.6	HRT III RCM	CCMetrics
Bitirgen et al. (Appendix S1)	Türkiye	Long COVID-19	45.6 ± 14.3	45.4 ± 13.1	16/14	22/18	19.2 ± 3.7	17.4 ± 4.6	HRT III RCM	CCMetrics
Bucher et al. [41]	Germany	SFN	61.0 ± 12.2	71.0 ± 9.8	7/7	7/7	22.9 ± 16.2	15.5 ± 22.2	HRT III RCM	ImageJ
Singh et al. [42]	Qatar	Celiac Disease	13.6 ± 1.3	12.7 ± 1.8	6/6	7/12	20 ± 4.5	19.8 ± 5.1	HRT III RCM	CCMetrics
Bussan et al. [43]	USA	OSA	59.9 ± 12.5	60.3 ± 14.8	14/12	19/17	11.1 ± 3.4	11.3 ± 3.0	HRT III RCM	MetaMorph
Gad et al. [44]	Qatar	Celiac Disease	12.8 ± 1.9	11.8 ± 1.74	11/9	7/13	19.5 ± 4.5	20.0 ± 5.1	HRT III RCM	CCMetrics

(Continues)

TABLE 1 | (Continued)

Study	Country	Condition	Age (years)		Sex (M/F)	CNFL (mm/mm^2)	CCM Model	Method
Midena et al. [45]	Italy	COVID-19	49.4 ± 26.5	56.8 ± 14.2	16/30	83/68	11.3 ± 3.6	11.9 ± 4.0	HRT III RCM	ACCMetrics
Moramarco et al. [46]	Italy	NF1	40.0 ± 15.0	46.0 ± 17.0	6/8	12/16	6.8 ± 3.9	7.9 ± 3.7	Confoscan3	*Not specified*
Canadas et al. [47]	Spain	Mercury Intoxication	42.0 ± 7.6	42.3 ± 7.3	22/0	22/0	14.5 ± 2.9	15.9 ± 4.5	HRT III RCM	ImageJ

Note: Age and CNFL data are presented in mean ± SD.

Abbreviations: AL amyloidosis, light chain amyloidosis; COVID-19, coronavirus disease 2019; CIDP, chronic inflammatory demyelinating polyradiculoneuropathy; CIPN, chemotherapy induced peripheral neuropathy; CMT1A, Charcot Marie Tooth type 1A; GI, gastrointestinal (cancer); HIV, human immunodeficiency virus; HTA, hereditary transthyretin amyloidosis; ISFN, idiopathic small fiber neuropathy; NF1, Neurofibromatosis Type 1; NGF-β, nerve growth factor-β; OSA, obstructive sleep apnea; SFN, small fiber neuropathy; SLE, systemic lupus erythematosus; TAO, thyroid disease associated ophthalmopathy; TFAP, transthyretin familial amyloid polyneuropathy.

From μm/frame to mm/mm^2.

- Conversion from μm to mm: (μm/1000).
- Image scale = 0.00104167 mm/pixel; image size = 384 × 384 pixels.
- Image width in mm = 384 × 0.00104167 = 0.4 mm; image height in mm = 384 × 0.00104167 = 0.4 mm; area in mm^2 = 0.4 × 0.4 = 0.16 mm^2.
- CNFL = mm/0.16mm^2.

2.5 | Data Synthesis and Analysis

Meta-analysis was undertaken with Review Manager (RevMan, Version 8.11.0, The Cochrane Collaboration, available at: https://revman.cochrane.org). A random effects model was employed for meta-analysis to account for heterogeneity between studies due to differences in study design and populations. The standardized mean difference (Hedge's adjusted g, Cochrane Handbook for Systematic Review and Interventions, Chapter 6, section 6.5.1.2) with a 95% confidence interval was calculated for CNFL and the chi-squared (χ^2) test was used to test for differences between subgroups. The I^2 statistic, derived from Cochrane's χ^2 test Q, was used to describe the between study variations attributed to variability in the true exposure effect. An I^2 value of 0%–40% was classified as not important, 30%–60% as moderate, 50%–90% as substantial, and 75%–100% as considerable. τ^2 with bias adjustment [τ^2 (DL^b)] was employed to estimate between-study variance when a random-effects model was used. To assess the effects of heterogeneity, sensitivity analysis was carried out to examine how the results of the meta-analysis change under different assumptions. Additionally, the results on fixed and random effects models were compared following the Cochrane recommendations (Cochrane Handbook for Systematic Review and Interventions, Chapter 10, section 10.4.4.1).

3 | Results

The search identified $n = 1904$ studies, of which $n = 654$ were removed as duplicates. Of the remaining $n = 1250$ potentially eligible studies, 996 studies were excluded, and 254 studies were selected for full-text review. Following full-text review, $n = 177$ studies were excluded as they did not fulfill our prespecified criteria (Figure 1). Seventy-seven studies were chosen for data extraction, of which a further $n = 25$ studies were removed due to lack of response by the authors. A total of $n = 52$ eligible studies reporting CNFL across 34 different conditions associated with PN were finally included. The detailed characteristics of all included studies are summarized in Tables 1–3. Altogether, there were $n = 2995$ participants classified into HC ($n = 1240$), PN+ ($n = 1526$), and PN− ($n = 229$). All studies included groups of HC and PN+ (Table 1), while $n = 9$ studies [10, 13, 14, 21, 23, 25, 31, 33, 35] further subdivided participants into PN− and PN+ (Tables 2 and 3). There were studies from Australia [25, 33, 35, 36], China [13, 27], France [12], Germany [20, 29, 30, 32, 40, 41], Hungary [24, 39], Italy [34, 45], Japan [18], the Netherlands [16, 22], Pakistan [17], Qatar [42, 44], Spain [11, 47], Sweden [10], Türkiye

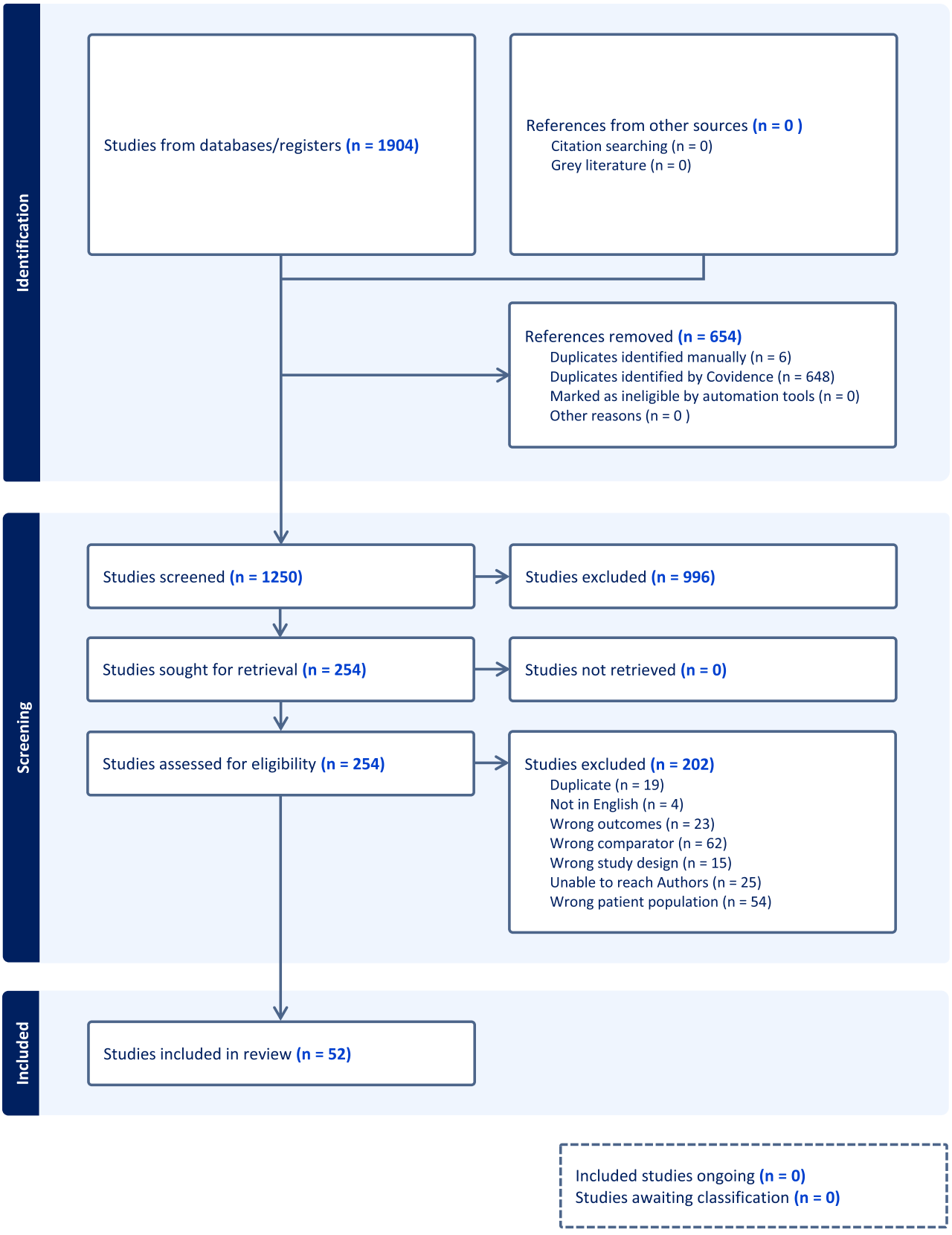

FIGURE 1 | Legend on next page.

FIGURE 1 | Study selection process flowchart according to the 2020 Preferred Reporting Items for Systematic Reviews and Meta-Analyses (PRISMA) statement. Studies were excluded for the following detailed reasons: Non-English ($n=1$ study was written in Bulgarian, $n=1$ study was written in Russian, $n=2$ studies were written in Chinese); wrong outcomes ($n=22$ studies did not include CNFL measurements, $n=1$ study assessed inter-observer variability); wrong comparator ($n=27$ studies did not include healthy controls as a comparator, $n=33$ studies did not include a disease group, $n=1$ study compared central cornea to the inferior whorl within the same group of patients, $n=1$ study compared patients on therapy versus no therapy without reference to the underlying neuropathy status); wrong study design ($n=8$ studies were case series; $n=5$ studies were clinical trials; $n=1$ study was a narrative review; $n=1$ study did not include a specific disease group); wrong patient population ($n=13$ studies were on patients with diabetes mellitus, $n=12$ studies were on patients with Parkinson's disease, $n=9$ were on patients with dry eye disease, $n=5$ studies were on patients with amyotrophic lateral sclerosis, $n=5$ studies were on patients with corneal neuropathic pain, $n=1$ study was on patients with congenital corneal anesthesia, $n=1$ study was on Sjögren's associated eye disease and did not specify the neuropathy status of patients, $n=1$ study was on patients with Bechet's disease with and without ocular findings and did not specify the neuropathy status of the non-ocular group, $n=1$ study was on patients with migraine, $n=1$ study was on patients with adult spinal dystrophy, $n=1$ study was on patients with burning mouth syndrome, $n=1$ study was on patients with trigeminal neuralgia, $n=1$ study was on patients with facial paralysis, $n=1$ study did not exclude diabetes, $n=1$ study was on patients with psychiatric disease).

[15, 19, 28, 38], (Appendix S1), the United Kingdom [21, 31], (Appendix S1) and the United States of America [26, 43], (Appendix S1). Most of the studies employed CCMetrics/ACCMetrics ($n=31$) for CCM image analysis, a smaller number used ImageJ/NeuronJ ($n=16$), MetaMorph ($n=1$), and device specific analysis tools (Tomey Confoscan P4), while $n=3$ studies did not specify the analysis method (Table 1). The included studies were published between 2010 and 2024.

3.1 | HC Versus PN+

We first examined CNFL across 34 different conditions with PN (PN+) (Table 1). Overall, CNFL was significantly lower in PN compared to HC (standardized mean difference −1.12, 95% confidence interval −1.32 to −0.33, $p<0.00001$) (Figure 2). In order of magnitude, the largest effect sizes were observed in patients with nerve growth factor-β mutation [10] (−4.64, −6.58 to −2.70), followed by fibromyalgia [11] (−4.13, −5.37 to −2.88), Sjögren's syndrome [12] (−2.50, −3.32 to −1.68), idiopathic small fiber neuropathy (Appendix S1) (−2.32, −3.29 to −1.34), upper gastrointestinal cancer (Appendix S1) (−2.17, −2.94 to −1.39), Charcot Marie Tooth Type 1A (Appendix S1) (−2.16, −3.21 to −1.12), and COVID-19 [14] (−1.95, −2.66 to −1.24). Conversely, no reliable effect sizes were observed in patients with obstructive sleep apnea [43] (0.06, −0.42 to 0.55), celiac disease [44] (0.10, −0.52 to 0.72), COVID-19 [45] (0.15, −0.18 to 0.48), neurofibromatosis type 1A [46] (0.29, −0.36 to 0.93), and mercury intoxication [47] (0.36, −0.24 to 0.96). There was considerable heterogeneity in the results [$\chi^2=271.56$, $p<0.00001$, $i^2=80\%$, τ^2 (DL^b)$=0.41$]. Twenty studies [11, 21, 22, 24, 25, 29, 30, 32, 35, 36, 39, 42, 45, 46], Appendix S1 were considered as "high" ($n=17$) or "unclear" ($n=3$) risk for detection bias. Sensitivity analysis showed that for the remaining studies ($n=827$ PN+; $n=750$ HC), CNFL was significantly lower in PN+ compared to HC (−1.17, −1.43 to −0.91, $p<0.00001$) and heterogeneity remained considerable [$\chi^2=155.52$, $p<0.00001$, $i^2=81\%$, τ^2 (DL^b)$=0.42$]. When a fixed instead of a random effects model was used, the overall results for CNFL (−0.99, −1.10 to −0.88, $p<0.00001$) remained significant and heterogeneity considerable ($\chi^2=155.52$, $p<0.00001$, $i^2=81\%$).

3.2 | HC Versus PN−

We examined CNFL in patients with sub-clinical PN (PN−) ($n=229$ PN− patients; $n=205$ HC) (Table 2). CNFL was significantly lower in PN− compared to HC (−0.78, −0.99 to −0.57, $p<0.00001$) (Figure 3). The largest effect size was observed in PN− patients with NGF-β mutation [10] (−2.70, −3.65 to −1.76), while there was no reliable effect size in patients on paclitaxel [33] (0.19–0.56 and 0.94). There was considerable heterogeneity in the results [$\chi^2=38.22$, $p<0.00001$, $i^2=79\%$, τ^2 (DL^b)$=0.40$]. Four studies [21, 25, 33, 35] were considered as "high" risk for detection bias. Sensitivity analysis showed that for the remaining studies ($n=122$ PN− patients; $n=101$ HC), CNFL differed significantly in PN− compared to HC (−1.22, −1.92 to −0.52, $p=0.0006$) and heterogeneity remained considerable [$\chi^2=19.52$, $p=0.0006$, $i^2=80\%$, τ^2 (DL^b)$=0.49$]. When a fixed instead of a random effects model was used, the overall results for CNFL remained significant (−0.78, −0.99 to −0.57, $p<0.00001$) and heterogeneity considerable ($\chi^2=263.82$, $p<0.00001$, $i^2=79\%$).

3.3 | PN− Versus PN+

Finally, we examined CNFL in 6 conditions with sub-clinical and clinical PN ($n=229$ PN− patients; $n=178$ PN+) (Table 3). CNFL was significantly lower in PN+ compared to PN− (−0.93, −1.53 to −0.33, $p=0.002$) (Figure 4). The largest effect size was observed in patients with nerve growth factor-β mutation [10] (−3.24, −4.93 to −1.55) followed by fibromyalgia [21] (−2.64, −3.66 to −1.63) and COVID-19 [21] (−1.69, −2.35 to −1.02), while no reliable effect size was observed between patients on two different chemotherapeutic agents [35] (paclitaxel vs. oxaliplatin) (0.17, −0.25 to 0.60). There was considerable heterogeneity in the results [$\chi^2=54.87$, $p<0.00001$, $i^2=85\%$, τ^2 (DL^b)$=0.68$]. Four studies [21, 25, 33, 35] were considered as "high" risk for detection bias. Sensitivity analysis showed that for the remaining studies ($n=74$ PN+ patients; $n=122$ PN− patients), CNFL differed significantly in PN+ compared to PN− patients (−0.99, −1.79 to −0.19, $p=0.02$) and heterogeneity remained considerable [$\chi^2=20.67$, $p=0.0004$, $i^2=81\%$, τ^2 (DL^b)$=0.63$]. When a fixed instead of a random effects model was used, the

TABLE 2 | Characteristics of studies for HC versus PN−.

Study	Country	Condition	Age (years)		Sex (M/F)		CNFL (mm/mm^2)		CCM Model	Method
			HC	PN−	HC	PN−	HC	PN−		
Perini et al. [10]	Sweden	NGF-β Mutation	49.9	52.5	9/10	9/7	23.6 + 5.1	11.5 ± 3.4	HRT III RCM	CCMetrics
Wu et al. [13]	China	TAO	44.1 ± 7.2	40.0 ± 7.6	7/13	5/19	17.6 ± 3.6	12.3 ± 3.1	HRT III RCM	ACCMetrics
Kemp et al. [31]	UK	HIV	53.8 ± 10.5	42.3 ± 7.3	20/0	6/0	27.2 ± 5.8	22.1 ± 3.1	HRT III RCM	CCMetrics
Chiang et al. [25]	Australia	CIPN	54.7 ± 12.6	58.3 ± 11.7	9/16	1/35	17.4 ± 3.6	13.8 ± 4.2	HRT III RCM	ACCMetrics
Chiang et al. [35]	Australia	CIPN	58.9 ± 7.9	58.6 ± 10.4	17/23	2/46	16.3 ± 3.2	13.1 ± 3.8	HRT III RCM	ACCMetrics
Mirza et al. [14]	Türkiye	COVID-19	35.5 ± 6.5	34.3 ± 7.9	16/6	12/12	17.8 ± 3.3	15.9 ± 2.1	HRT III RCM	ImageJ
Luzu et al. [23]	France	Sjögren's syndrome	50.9 ± 21.8	58.0 ± 12.5	6/14	6/46	20.5 ± 3.1	17.3 ± 6.9	HRT III RCM	ImageJ
Chiang et al. [33]	Australia	CIPN	52.1 ± 14.0	42.3 ± 10.1	2/27	0/9	16.4 ± 4.0	17.2 ± 4.3	HRT III RCM	ACCMetrics
Marshall et al. [21]	UK	Fibromyalgia	42.6 ± 11.8	42.4 ± 14.8	1/9	1/14	16.0 ± 3.0	17.1 ± 1.5	HRT III RCM	ACCMetrics

Note: Age and CNFL data are presented in mean ± SD.
Abbreviations: CIPN, chemotherapy induced peripheral neuropathy; HIV, human immunodeficiency virus; NGF-β, nerve growth factor-β; TAO, thyroid disease associated ophthalmopathy.

TABLE 3 | Characteristics of studies for PN− versus PN+.

Study	Country	Condition	Age (years)		Sex (M/F)		CNFL (mm/mm^2)		CCM Model	Method
			PN−	PN+	PN−	PN+	PN−	PN+		
Perini et al. [10]	Sweden	NGF-β Mutation	52.5	40.3	9/7	2/1	11.5 ± 3.4	0.5 ± 0.8	HRT III RCM	CCMetrics
Marshall et al. [21]	UK	Fibromyalgia	42.4 ± 14.8	45.4 ± 15.0	1/14	1/14	17.1 ± 1.5	12.3 ± 2.0	HRT III RCM	ACCMetrics
Mirza et al. [14]	Türkiye	COVID-19	34.3 ± 7.9	36.7 ± 8.3	12/12	12/12	15.9 ± 2.1	11.6 ± 2.9	HRT III RCM	ImageJ
Chiang et al. [33]	Australia	CIPN	42.3 ± 10.1	58.7 ± 10.4	0/9	2/18	17.2 ± 4.3	12.9 ± 3.0	HRT III RCM	ACCMetrics
Wu et al. [13]	China	TAO	40.0 ± 7.6	43.5 ± 5.7	5/19	5/9	12.3 ± 3.1	10.4 ± 3.0	HRT III RCM	ACCMetrics
Luzu et al. [23]	France	Sjögren's syndrome	58.0 ± 12.5	67.1 ± 7.9	6/46	2/17	17.3 ± 6.9	15.0 ± 5.2	HRT III RCM	ImageJ
Chiang et al. [25]	Australia	CIPN	58.3 ± 11.7	61.9 ± 10.7	1/35	14/16	13.8 ± 4.2	13.1 ± 3.2	HRT III RCM	ACCMetrics
Kemp et al. [31]	UK	HIV	42.3 ± 7.3	57.7 ± 7.8	6/0	14/0	22.1 ± 3.1	22.2 ± 3.6	HRT III RCM	CCMetrics
Chiang et al. [35]	Australia	CIPN	58.6 ± 10.4	60.8 ± 9.5	2/46	21/18	13.1 ± 3.8	13.7 ± 2.9	HRT III RCM	ACCMetrics

Note: Age and CNFL data are presented in mean ± SD.
Abbreviations: CIPN, chemotherapy induced peripheral neuropathy; HIV, human immunodeficiency virus; NGF-β, nerve growth factor-β; TAO, thyroid disease associated ophthalmopathy.

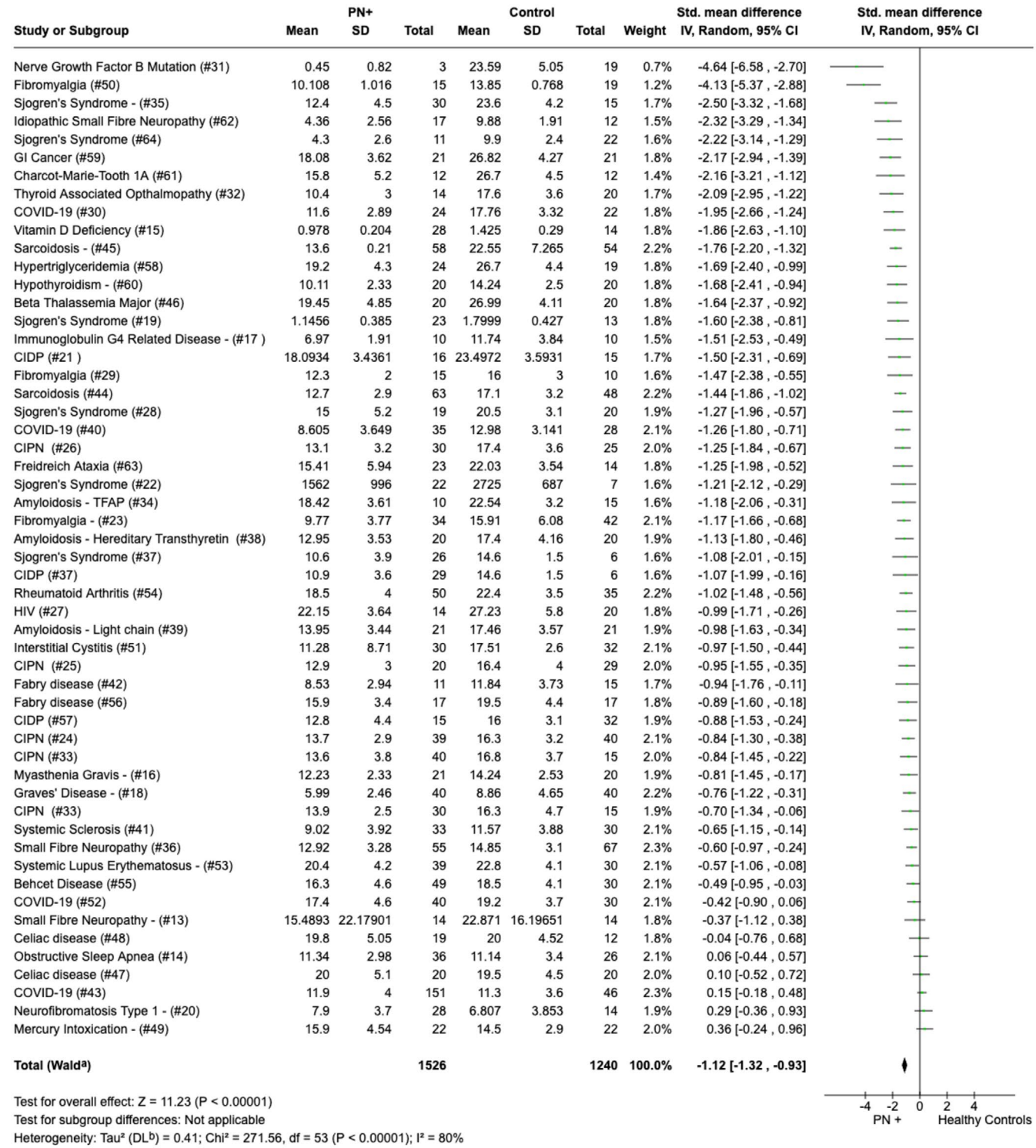

Footnotes

[a]CI calculated by Wald-type method.

[b]Tau² calculated by DerSimonian and Laird method.

FIGURE 2 | Forest plot of meta-analysis comparing CNFL in patients with clinically detectable peripheral neuropathy (PN+) to healthy controls (HC). A random-effects model was used. Outcomes are expressed as standardized mean difference (SMD) with a 95% confidence interval. The overall effect size is expressed with a *Z* score (*p*-value); and heterogeneity is expressed with τ, coefficients, and i^2. Risk of bias was assessed on four categories (D: detection bias; E: attrition bias; F: reporting bias; and G: other bias) and is shown on the right. Categories A–C (selection, performance bias) are relevant to clinical trials and in the present meta-analysis were considered not applicable. Sensitivity analysis not shown in this graph.

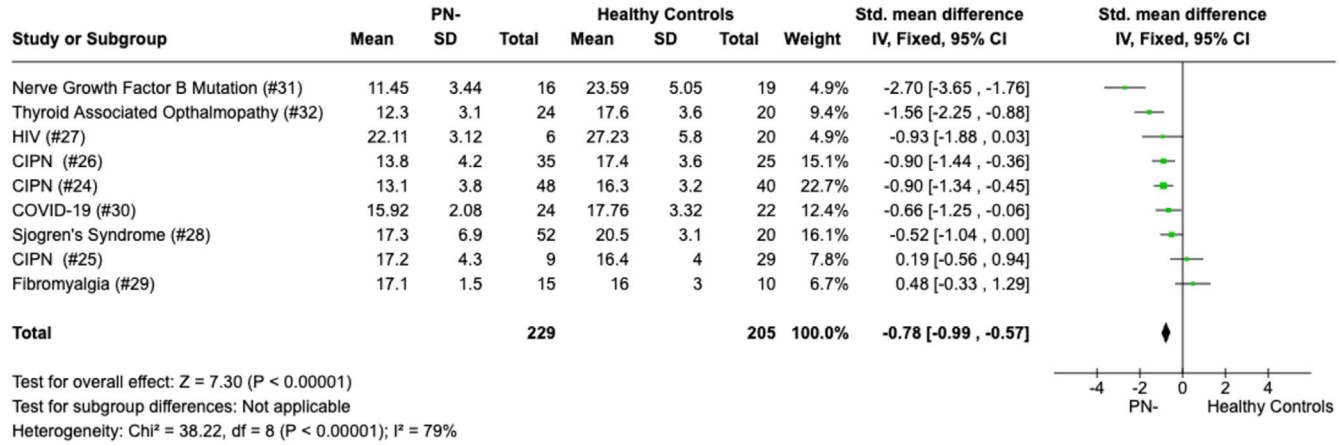

FIGURE 3 | Forest plot of meta-analysis comparing CNFL in patients without clinically detectable peripheral neuropathy (PN−) to HC. A random-effects model was used. Outcomes are expressed as standardized mean difference (SMD) with a 95% confidence interval. The overall effect size is expressed with a Z score (p-value); and heterogeneity is expressed with τ, coefficients, and i^2. Risk of bias was assessed on four categories (D: detection bias; E: attrition bias; F: reporting bias; and G: other bias) and is shown on the right. Categories A–C (selection, performance bias) are relevant to clinical trials and, in the present meta-analysis, were considered not applicable. Sensitivity analysis not shown in this graph.

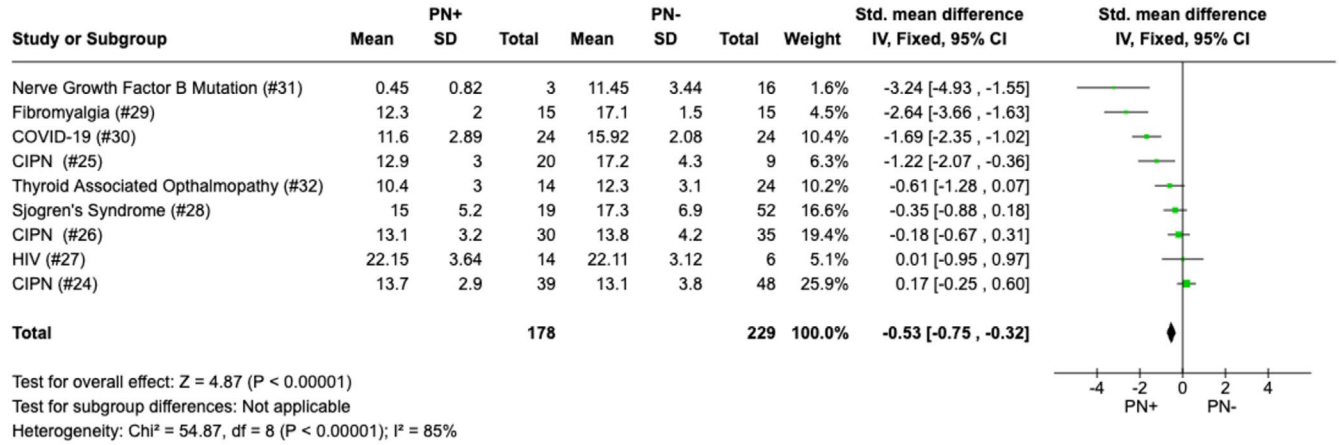

FIGURE 4 | Forest plot of meta-analysis comparing CNFL in PN+ to PN− patients. A random-effects model was used. Outcomes are expressed as standardized mean difference (SMD) with 95% confidence interval. The overall effect size is expressed with Z score (p-value); and heterogeneity is expressed with τ, coefficients, and i^2. Risk of bias was assessed on four categories (D: detection bias; E: attrition bias; F: reporting bias; and G: other bias) and is shown on the right. Categories A–C (selection, performance bias) are relevant to clinical trials and in the present meta-analysis were considered not applicable. Sensitivity analysis is not shown in this graph.

overall results for CNFL remained significant (−0.53, −0.75 to −0.32, $p<0.00001$) and heterogeneity considerable ($\chi^2=54.87$, $p<0.00001$, $i^2=85\%$).

3.4 | Sjögren's Syndrome

Six studies [12, 18, 23, 26, 30], [64] estimated CNFL in patients with Sjögren's syndrome and PN compared to HC ($n=131$ Sjögren's syndrome; $n=82$ HC) (Figure 5). CNFL was significantly lower in patients with Sjögren's syndrome and PN compared to HC (−1.64, −2.1 to −1.18, $p<0.00001$). There was moderate heterogeneity in the results [$\chi^2=9.05$, $p=0.11$, $i^2=45\%$, τ^2 (DL^b)$=0.15$]. Two studies [37, 64] were considered as "high" risk for detection bias. Sensitivity analysis showed that for the remaining studies ($n=94$ Sjögren's patients with PN; $n=55$ HC), CNFL was significantly lower (−1.64, −2.21 to −1.07, $p<0.00001$) and heterogeneity remained moderate [$\chi^2=6.16$, $p=0.10$, $i^2=51\%$, τ^2 (DL^b)$=0.17$]. When a fixed instead of a random effects model was used, the overall results for CNFL remained significant (−1.63, −1.97 to −1.29, $p<0.00001$) and heterogeneity moderate ($\chi^2=9.05$, $p<0.00001$, $i^2=45\%$).

4 | Discussion

In this meta-analysis of 2995 participants, CNFL was significantly lower in PN+ patients compared to HC and PN− patients. Furthermore, CNFL was significantly lower in PN−patients compared to HC. The largest effect sizes were observed in patients with NGF-β mutation [10], fibromyalgia [11], Sjögren's syndrome [12], gastrointestinal cancer (Appendix S1), and Charcot Marie Tooth type 1A neuroarthropathy (Appendix S1). Several other peripheral neuropathies of genetic, metabolic,

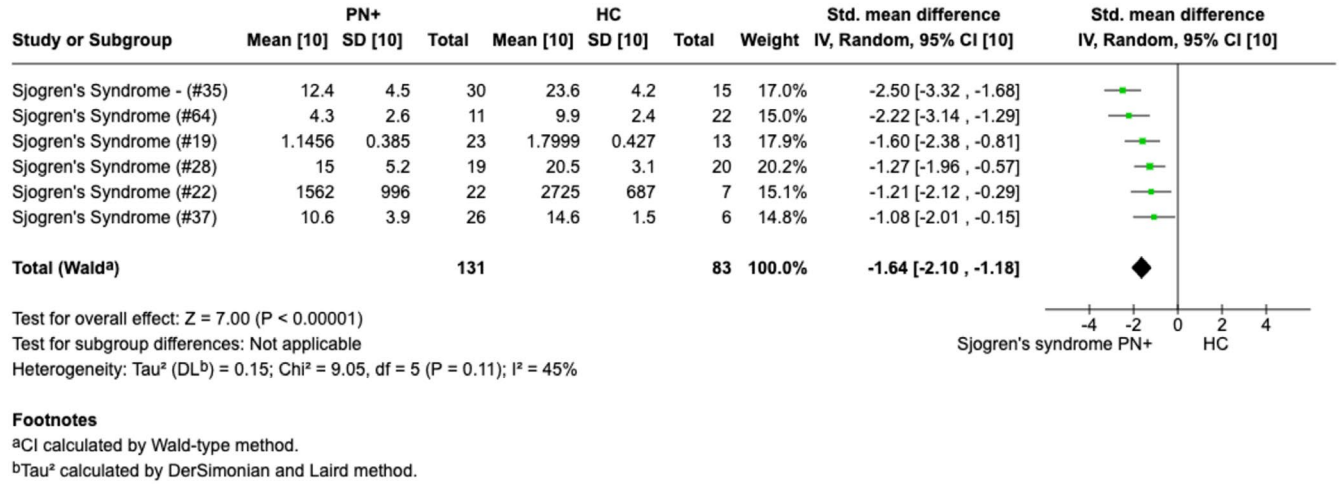

FIGURE 5 | Forest plot of meta-analysis comparing CNFL in patients with Sjögren's syndrome and clinically detectable PN to HC. A random-effects model was used. Outcomes are expressed as standardized mean difference (SMD) with a 95% confidence interval. The overall effect size is expressed with a Z score (p-value); and heterogeneity is expressed with τ, coefficients, and i^2. Risk of bias was assessed on four categories (D: detection bias; E: attrition bias; F: reporting bias; and G: other bias) and is shown on the right. Categories A–C (selection, performance bias) are relevant to clinical trials and in the present meta-analysis were considered not applicable. Sensitivity analysis is not shown in this graph.

toxic, autoimmune, or inflammatory origin produced smaller, albeit significant, effect sizes. By contrast, studies in patients with obstructive sleep apnea [43], neurofibromatosis type 1 [46], celiac disease [44], and mercury intoxication [47] showed no reliable effect sizes for the detection of PN by CCM. COVID-19 produced variable effect sizes depending on the study [14, 24, 45], (Appendix S1), likely reflecting differences in the underlying study cohort, diagnostic definitions, disease duration, and severity. Our findings are in agreement with previous meta-analyses showing the utility of CCM as a biomarker of diabetic PN (Appendix S1), and as an outcome measure in clinical trials of neuroregenerative treatments (Appendix S1).

PN is a highly heterogeneous and underdiagnosed neurological condition due to many common and rare systemic disorders. Epidemiological data on the prevalence of PN are limited in part due to a lack of uniform diagnostic criteria [1], (Appendix S1). The prevalence of diabetic neuropathy (Appendix S1), Guillain-Barre syndrome (Appendix S1), and Charcot–Marie–Tooth disease (Appendix S1) varies by region and diagnostic methodology. PN can be diagnosed based on symptoms and confirmed by objective tests such as quantitative sensory testing, neurophysiology, and skin biopsy (Appendix S1). Degeneration of small unmyelinated axons in a dying-back pattern, and sensory symptoms are common features of most metabolic, toxic, and nutritional neuropathies (Appendix S1). Evaluation of intra-epidermal nerve fiber density provides an accurate and sensitive approach to confirm small fiber neuropathy, but it is invasive and not widely available, particularly in resource-limited settings (Appendix S1).

An increasing body of evidence shows that quantification of CNFL may serve as a sensitive biomarker for small nerve fiber damage and repair. CCM is a high resolution, high magnification (600×), non-invasive laser scanning microscope for real-time optical biopsies of the entire cornea at the cellular level, including the subbasal nerve plexus. The cornea shares pathophysiological similarities with the skin and is densely innervated with subbasal C-fibers [4], which originate from the ophthalmic division of the trigeminal ganglion. It is estimated that the cornea contains approximately 11,000 axonal endings/mm^2, thus making it one of the most densely innervated tissues of the human body (Appendix S1). Corneal C-fibers degenerate in sub-clinical disease (Appendix S1); decline with increasing severity (Appendix S1); and regenerate early following therapy (Appendix S1). Furthermore, visualizing corneal nerve fibers with CCM can be done repeatedly and requires minimal technical aptitude. This is the first systematic review and meta-analysis to provide an overall estimate of the ability of CCM to identify small nerve fiber damage in patients with clinical peripheral neuropathy (PN+), and sub-clinical peripheral neuropathy (PN−). Two recent studies have challenged the diagnostic utility of CCM in diabetic neuropathy by showing lower sensitivity and similar specificity compared to intra-epidermal nerve fiber density (Appendix S1). Curiously, even intra-epidermal nerve fiber density, the gold standard measure of small fiber neuropathy, showed overall modest diagnostic performance, suggesting limitations with the case definition of PN, which was large-fiber weighted (Appendix S1). Methodological differences in CCM image quantification and diagnostic performance analysis may have also led to these results. Nevertheless, the present meta-analysis suggests potential utility of CCM in the diagnosis of a wide range of peripheral neuropathies, although diagnostic performance remains to be established in the respective conditions.

We observed a significant difference in the magnitude of CNFL differences between studies amongst all subgroups (PN+ vs. HC, PN+ vs. PN−, and PN− vs. HC) indicating that the extent of corneal nerve loss may depend on several factors. Thus, age and disease severity may result in varying degrees of axonal loss (Appendix S1). Studies in healthy persons have shown an age-dependent decline in corneal subbasal nerves (Appendix S1). Chin et al. (Appendix S1) demonstrated a significant decline in CNFL in persons older than 65 years, while Tavakoli et al. (Appendix S1) showed a decline across the life span, particularly in women, which was not related to established cardiovascular

risk factors. Disease severity is another factor that has been strongly associated with corneal axonal loss. Indeed, a previous study has shown lower CNFL in patients with rheumatoid arthritis and higher disease activity (Appendix S1); while in patients with sarcoidosis-induced painful neuropathy (Appendix S1) and diabetic painful neuropathy (Appendix S1), CNFL was inversely related to pain intensity. In Parkinson's disease, a central condition with known peripheral nerve involvement, a lower CNFL has been associated with postural instability and gait disturbance compared to the tremor-dominant motor subtype (Appendix S1). In the longitudinal setting, accelerated CNFL loss in patients with diabetes is associated with higher odds of neuropathy onset and progression at follow-up compared to baseline [90]. In the present meta-analysis, we observed significant variation in CNFL across diseases and the effect of differences in age on CNFL across these diseases is unclear. Additionally, study-specific reasons such as the imaging technique and analysis method may have also impacted the outcome. Currently, there is a lack of standardized methodology for CCM image acquisition and analysis. Different centers may scan the central subbasal (Appendix S1) and inferior whorl regions (Appendix S1); a predefined region of interest (Appendix S1); or even generate corneal nerve maps (Appendix S1). Consequently, images for analysis may also differ, representing a single "best" image (Appendix S1), a sample of images (Appendix S1), or a map (Appendix S1). Lastly, we found moderate to considerable heterogeneity in the reported outcomes between studies, potentially reflecting the lack of a uniformly applicable definition of PN as well as differences in study design and diagnostic modalities used. Interestingly, there was lower heterogeneity when comparing only studies in Sjögren's syndrome as evidenced by lower between-study variance indicating a more consistent approach within a single disease area.

Our study has some limitations. First, the case definition of PN may differ between studies and since we had no access to the underlying study data, we could not apply uniform diagnostic criteria but had to rely on the published results. This may have resulted in over- or underestimation of PN cases in the study cohort, which could potentially affect the observed differences. Second, we could not analyze the full spectrum of eligible studies due to lack of adequate details for inclusion. Finally, we included studies that used only a specific type of CCM in an attempt to reduce heterogeneity due to differences in image acquisition and resolution. In conclusion, CNFL was consistently lower in patients with clinical and sub-clinical neuropathy. Given that CCM is rapid, non-invasive, and objective, it has considerable clinical utility as a sensitive diagnostic test for PN.

Author Contributions

Ioannis N. Petropoulos: conceptualization (lead), resources (lead), methodology (lead), software (lead), data curation (equal), formal analysis (equal), investigation (equal), supervision (lead), visualization (equal), and writing – original draft preparation (lead). **Omar A. Madani:** data curation (equal), formal analysis (equal), investigation (equal), visualization (equal), and writing – original draft preparation (equal). **Hoda Y. Gad:** software (equal), data curation (equal), investigation (equal), and writing – review and editing (equal). **Georgios Ponirakis:** data curation (equal), and writing – review and editing (equal). **Ziyad R. Mahfoud:** formal analysis (equal), validation (equal), and writing – review and editing (equal). **Ross MacDonald:** resources (lead), methodology (lead), software (lead), and writing – review and editing (equal). **Rayaz A. Malik:** funding acquisition (lead), resources (lead), supervision (equal), and writing – review and editing (lead).

Conflicts of Interest

The authors declare no conflicts of interest.

Data Availability Statement

The data that support the findings of this study are available from the corresponding author upon reasonable request.

References

1. C. Martyn and R. Hughes, "Epidemiology of Peripheral Neuropathy," *Journal of Neurology, Neurosurgery, and Psychiatry* 62 (1997): 310–318.

2. E. Hoitsma, J. P. H. Reulen, M. de Baets, M. Drent, F. Spaans, and C. G. Faber, "Small Fiber Neuropathy: A Common and Important Clinical Disorder," *Journal of the Neurological Sciences* 227 (2004): 119–130.

3. G. Lauria, S. T. Hsieh, O. Johansson, et al., "European Federation of Neurological Societies/Peripheral Nerve Society Guideline on the Use of Skin Biopsy in the Diagnosis of Small Fiber Neuropathy. Report of a Joint Task Force of the European Federation of Neurological Societies and the Peripheral Nerve Society," *European Journal of Neurology* 17 (2010): 903–e949.

4. E. A. Moulton and D. Borsook, "C-Fiber Assays in the Cornea vs. Skin," *Brain Sciences* 9 (2019): 320.

5. R. A. Malik, P. Kallinikos, C. Abbott, et al., "Corneal Confocal Microscopy: A Non-Invasive Surrogate of Nerve Fibre Damage and Repair in Diabetic Patients," *Diabetologia* 46 (2003): 683–688.

6. M. E. Rosenberg, T. M. Tervo, I. J. Immonen, L. J. Müller, C. Grönhagen–Riska, and M. H. Vesaluoma, "Corneal Structure and Sensitivity in Type 1 Diabetes Mellitus," *Investigative Ophthalmology & Visual Science* 41 (2000): 2915–2921.

7. I. N. Petropoulos, G. Bitirgen, M. Ferdousi, et al., "Corneal Confocal Microscopy to Image Small Nerve Fiber Degeneration: Ophthalmology Meets Neurology," *Frontiers in Pain Research* 2 (2021): 725363.

8. D. Moher, A. Liberati, J. Tetzlaff, D. G. Altman, and Group P, "Preferred Reporting Items for Systematic Reviews and Meta-Analyses: the PRISMA Statement," *International Journal of Surgery* 8 (2010): 336–341.

9. H. Gad, I. N. Petropoulos, A. Khan, et al., "Corneal Confocal Microscopy for the Diagnosis of Diabetic Peripheral Neuropathy: A Systematic Review and Meta-Analysis," *Journal of Diabetes Investigation* 13 (2022): 134–147.

10. I. Perini, M. Tavakoli, A. Marshall, J. Minde, and I. Morrison, "Rare Human Nerve Growth Factor-β Mutation Reveals Relationship Between C-Afferent Density and Acute Pain Evaluation," *Journal of Neurophysiology* 116 (2016): 425–430.

11. J. Q. Piñeiro, A. Barros, J. Lozano-Sanroma, et al., "Confocal Microscopy In Vivo in Patients Diagnosed With Fibromyalgia," *Investigative Ophthalmology & Visual Science* 63 (2022): 1205.

12. O. Levy, A. Labbé, V. Borderie, et al., "Increased Corneal Sub-Basal Nerve Density in Patients With Sjögren Syndrome Treated With Topical Cyclosporine A," *Clinical & Experimental Ophthalmology* 45 (2017): 455–463.

13. L.-Q. Wu, P. Mou, Z.-Y. Chen, et al., "Altered Corneal Nerves in Chinese Thyroid-Associated Ophthalmopathy Patients Observed by In Vivo Confocal Microscopy," *Medical Science Monitor: International Medical Journal of Experimental and Clinical Research* 25 (2019): 1024–1031.

14. E. Mirza, S. Belviranli, A. O. Gundogan, M. Adam, and R. Oltulu, "Quantitative Assessment of the Effect of SARS-CoV-2 on the Corneal

Sub-Basal Nerve Plexus of Post-COVID-19 Patients Using In Vivo Confocal Microscopy," *Eye* 37 (2023): 660–664.

15. N. Ç. Başaran, D. Kırağı, Ç. Tan, et al., "Ocular Changes and Tear Cytokines in Individuals With Low Serum Vitamin D Levels: A Cross-Sectional, Controlled Study," *Ocular Immunology and Inflammation* 32 (2024): 287–294.

16. L. C. J. Oudejans, M. Niesters, M. Brines, A. Dahan, and M. van Velzen, "Quantification of Small Fiber Pathology in Patients With Sarcoidosis and Chronic Pain Using Cornea Confocal Microscopy and Skin Biopsies," *Journal of Pain Research* 10 (2017): 2057–2065.

17. S. A. Khan, S. A. H. Naqvi, A. Saeed, et al., "Peripheral Neuropathy in Beta-Thalassemia: Corneal Confocal Microscopy-Based Study," *Cureus* 14 (2022): e32122.

18. Y. Matsumoto, O. M. Ibrahim, T. Kojima, M. Dogru, J. Shimazaki, and K. Tsubota, "Corneal In Vivo Laser-Scanning Confocal Microscopy Findings in Dry Eye Patients With Sjögren's Syndrome," *Diagnostics* 10 (2020): 497.

19. S. Kocabeyoglu, O. Karadag, M. C. Mocan, A. Erden, and M. Irkec, "Orbital Involvement and Ocular Surface Changes in IgG4-Related Systemic Disease," *Cornea* 35 (2016): 1449–1453.

20. C. Schneider, F. Bucher, C. Cursiefen, G. R. Fink, L. M. Heindl, and H. C. Lehmann, "Corneal Confocal Microscopy Detects Small Fiber Damage in Chronic Inflammatory Demyelinating Polyneuropathy (CIDP)," *Journal of the Peripheral Nervous System* 19 (2014): 322–327.

21. A. Marshall, L. Rapteas, J. Burgess, et al., "Small Fibre Pathology, Small Fibre Symptoms and Pain in Fibromyalgia Syndrome," *Scientific Reports* 14 (2024): 3947.

22. M. Brines, D. A. Culver, M. Ferdousi, et al., "Corneal Nerve Fiber Size Adds Utility to the Diagnosis and Assessment of Therapeutic Response in Patients With Small Fiber Neuropathy," *Scientific Reports* 8 (2018): 4734.

23. J. Luzu, A. Labbé, A. Réaux-Le Goazigo, et al., "In Vivo Confocal Microscopic Study of Corneal Innervation in Sjögren's Syndrome With or Without Small Fiber Neuropathy," *Ocular Surface* 25 (2022): 155–162.

24. Z. Kolkedi, A. Csutak, and E. Szalai, "Analysis of Microvascular and Neurodegenerative Complications of Mild COVID-19," *Graefe's Archive for Clinical and Experimental Ophthalmology* 260 (2022): 2687–2693.

25. J. C. B. Chiang, D. Goldstein, T. Trinh, et al., "Tear Film Substance P in Patients Treated With Neurotoxic Chemotherapy," *Experimental Eye Research* 224 (2022): 109253.

26. T. C. Tepelus, G. B. Chiu, J. Huang, et al., "Correlation Between Corneal Innervation and Inflammation Evaluated With Confocal Microscopy and Symptomatology in Patients With Dry Eye Syndromes: a Preliminary Study," *Graefe's Archive for Clinical and Experimental Ophthalmology* 255 (2017): 1771–1778.

27. Y. Zhang, Z. Liu, Y. Zhang, et al., "Corneal Sub-Basal Whorl-Like Nerve Plexus: A Landmark for Early and Follow-Up Evaluation in Transthyretin Familial Amyloid Polyneuropathy," *European Journal of Neurology* 28 (2021): 630–638.

28. K. E. Turan, S. Kocabeyoglu, I. Unal-Cevik, F. Bezci, A. Akinci, and M. Irkec, "Ocular Surface Alterations in the Context of Corneal In Vivo Confocal Microscopic Characteristics in Patients With Fibromyalgia," *Cornea* 37 (2018): 205–210.

29. A. Thimm, A. Carpinteiro, S. Oubari, et al., "Corneal Confocal Microscopy Identifies Corneal Nerve Loss and Increased Langerhans Cells in Presymptomatic Carriers and Patients With Hereditary Transthyretin Amyloidosis," *Journal of Neurology* 270 (2023): 3483–3491.

30. T. Seeliger, M. A. Gehlhaar, I. Oluwatoba-Popoola, et al., "Trigeminal Nerve Affection in Patients With Neuro-Sjögren Detected by Corneal Confocal Microscopy," *Journal of Clinical Medicine* 11 (2022): 4484.

31. H. I. Kemp, I. N. Petropoulos, A. S. C. Rice, et al., "Use of Corneal Confocal Microscopy to Evaluate Small Nerve Fibers in Patients With Human Immunodeficiency Virus," *JAMA Ophthalmology* 135 (2017): 795–800.

32. A. Thimm, A. Carpinteiro, S. Oubari, et al., "Corneal Confocal Microscopy to Detect Early Immune-Mediated Small Nerve Fibre Loss in AL Amyloidosis," *Annals of Clinical and Translational Neurology* 9 (2022): 853–863.

33. J. C. B. Chiang, D. Goldstein, T. Trinh, et al., "A Cross-Sectional Study of Ocular Surface Discomfort and Corneal Nerve Dysfunction After Paclitaxel Treatment for cancer," *Scientific Reports* 11 (2021): 1786.

34. M. Marenco, M. Segatto, M. Sacchetti, P. Mangiantini, F. Giovannetti, and R. Plateroti, "Autophagy-Lysosome Pathway Alteration in Ocular Surface Manifestations in Fabry Disease Patients," *Orphanet Journal of Rare Diseases* 17 (2022): 291.

35. J. Chiang, M. Markoulli, T. Trinh, et al., "Chemotherapy-Induced Peripheral Neuropathy With Evidence of Corneal Nerve Loss and Dendritic Cell Increase: A Cross-Sectional Study," *Supportive Care in Cancer* 29 (2021): S1–S261.

36. J. C. B. Chiang, D. Goldstein, T. Trinh, et al., "A Cross-Sectional Study of Sub-Basal Corneal Nerve Reduction Following Neurotoxic Chemotherapy," *Translational Vision Science & Technology* 10 (2021): 24.

37. K. E. Turan, S. Kocabeyoglu, C. E. Bekircan-Kurt, F. Bezci, S. Erdem-Ozdamar, and M. Irkec, "Ocular Surface Alterations and In Vivo Confocal Microscopic Characteristics of Corneas in Patients With Myasthenia Gravis," *European Journal of Ophthalmology* 28 (2018): 541–546.

38. S. Kocabeyoglu, M. C. Mocan, Y. Cevik, and M. Irkec, "Ocular Surface Alterations and In Vivo Confocal Microscopic Features of Corneas in Patients With Newly Diagnosed Graves' Disease," *Cornea* 34 (2015): 745–749.

39. E. Szalai, G. Szucs, S. Szamosi, Z. Aszalos, I. Afra, and A. Kemeny-Beke, "An In Vivo Confocal Microscopy Study of Corneal Changes in Patients With Systemic Sclerosis," *Scientific Reports* 11 (2021): 11111.

40. N. Egenolf, C. M. Altenschildesche, L. Kreß, et al., "Diagnosing Small Fiber Neuropathy in Clinical Practice: A Deep Phenotyping Study," *Therapeutic Advances in Neurological Disorders* 14 (2021): 17562864211004318.

41. F. Bucher, C. Schneider, T. Blau, et al., "Small-Fiber Neuropathy Is Associated With Corneal Nerve and Dendritic Cell Alterations: An In Vivo Confocal Microscopy Study," *Cornea* 34 (2015): 1114–1119.

42. P. Singh, A. Rawat, B. Al-Jarrah, et al., "Distinctive Microbial Signatures and Gut-Brain Crosstalk in Pediatric Patients With Coeliac Disease and Type 1 Diabetes Mellitus," *International Journal of Molecular Sciences* 22 (2021): 1511.

43. K. A. Bussan, W. L. Stuard, N. Mussi, et al., "Differential Effects of Obstructive Sleep Apnea on the Corneal Subbasal Nerve Plexus and Retinal Nerve Fiber Layer," *PLoS One* 17 (2022): e0266483.

44. H. Gad, S. Saraswathi, B. Al-Jarrah, et al., "Corneal Confocal Microscopy Demonstrates Minimal Evidence of Distal Neuropathy in Children With Celiac Disease," *PLoS One* 15 (2020): e0238859.

45. E. Midena, E. Cosmo, A. M. Cattelan, et al., "Small Fibre Peripheral Alterations Following COVID-19 Detected by Corneal Confocal Microscopy," *Journal of Personalized Medicine* 12 (2022): 563.

46. A. Moramarco, M. Sacchetti, F. Franzone, et al., "Ocular Surface Involvement in Patients With Neurofibromatosis Type 1 Syndrome," *Graefe's Archive for Clinical and Experimental Ophthalmology* 258 (2020): 1757–1762.

47. P. Cañadas, Y. Lantigua, A. Enríquez-de-Salamanca, et al., "Ocular Surface Pathology in Patients Suffering From Mercury Intoxication," *Diagnostics* 11 (2021): 1326.

48. J. Shi, D. Luo, H. Weng, et al., "Optimally Estimating the Sample Standard Deviation From the Five-Number Summary," *Research Synthesis Methods* 11 (2020): 641–654.

49. D. Luo, X. Wan, J. Liu, and T. Tong, "Optimally Estimating the Sample Mean From the Sample Size, Median, Mid-Range, and/or Mid-Quartile Range," *Statistical Methods in Medical Research* 27 (2018): 1785–1805.

50. X. Wan, W. Wang, J. Liu, and T. Tong, "Estimating the Sample Mean and Standard Deviation From the Sample Size, Median, Range and/or Interquartile Range," *BMC Medical Research Methodology* 14 (2014): 135.

References 51 to 97 are cited in Supporting Information.

Supporting Information

Additional supporting information can be found online in the Supporting Information section. **Figure S1:** CCM allows rapid, live, non-invasive scanning of the human cornea. This montage of CCM images shows a typical CCM scan, which captures superficial (A) and basal (B) epithelial cells, subbasal C-fibers (C–I), stromal keratocytes (J–L), and endothelial cells (M). **Table S1:** Database search strings. **Appendix S1:** ene70396-sup-0003-AppendixS1.docx.